Pressure dependence of the optical properties of the charge-density-wave compound $LaTe_2$

M. Lavagnini, A. Sacchetti, and L. Degiorgi
Laboratorium für Festkörperphysik, ETH-Zürich, CH-8093 Zürich, Switzerland

E. Arcangeletti, L. Baldassarre, P. Postorino, and S. Lupi
CNR-INFM-Coherentia and Dipartimento di Fisica, Università "La Sapienza," Piazzale Aldo Moro 5, I-00185 Rome, Italy

A. Perucchi
CNR-INFM-Coherentia and Sincrotrone Trieste, Area Science Park, Basovizza, I-34012 Trieste, Italy

K. Y. Shin and I. R. Fisher
Geballe Laboratory for Advanced Materials and Department of Applied Physics, Stanford University, Stanford, California 94305-4045, USA

(Received 12 December 2007; revised manuscript received 16 March 2008; published 29 April 2008)

We report the pressure dependence of the optical response of $LaTe_2$, which is deep in the charge-density-wave (CDW) ground state even at 300 K. The reflectivity spectrum is collected in the midinfrared spectral range at room temperature and at pressures between 0 and 7 GPa. We extract the energy scale due to the single-particle excitation across the CDW gap and the Drude weight. We establish that the gap decreases upon compressing the lattice while the Drude weight increases. This signals a reduction in the quality of nesting upon applying pressure, therefore inducing a lesser impact of the CDW condensate on the electronic properties of $LaTe_2$. The consequent suppression of the CDW gap leads to a release of additional charge carriers, manifested by the shift of weight from the gap feature into the metallic component of the optical response. On the contrary, the power-law behavior, seen in the optical conductivity at energies above the gap excitation and indicating a weakly interacting limit within the Tomonaga-Luttinger liquid scenario, seems to be only moderately dependent on pressure.

DOI: 10.1103/PhysRevB.77.165132 PACS number(s): 71.45.Lr, 78.20.−e, 07.35.+k

I. INTRODUCTION

Peierls was the first, in the early sixties, to predict the formation of a charge-density-wave (CDW) ground state for one-dimensional (1D) metals when turning on the electron-phonon interaction.[1] The CDW phase transition relates to a balance between electronic energy and lattice structural stability. For 1D metals, it is energetically favorable to introduce a lattice distortion which, combined with a so-called Fermi-surface (FS) nesting, leads to a novel collective charge ordering. The formation of the CDW condensate implies the opening of a gap on the FS and therefore the lowering of the overall electronic energy.[1,2] Several families of materials, including the transition-metal di- and trichalcogenides, the molybdenum and tungsten oxides such as the blue and purple bronzes, and the organic charge transfer salts, were then discovered after Peierls' pioneering theoretical prediction and intensively studied over several decades.[2,3]

The discovery of superconductivity at high temperature in the low-dimensional layered-like cuprates also induces a revival of interest in the prototype CDW systems because they provide excellent opportunities for theoretical investigation toward how strongly correlated electron-phonon systems behave and how electron-phonon interaction affects the band structure. In this context, the rare-earth polychalcogenide RTe_n (R stands for rare earth, and $n=2$, 2.5, and 3) systems have attracted a great deal of interest due to their intrinsic low dimensionality. These materials are also characterized by a layered structure, consisting of corrugated rare-earth-chalcogen slabs alternated with planar chalcogen square lattices (i.e., single layer for di- and double layer for tritellurides).[4] This crystal structure shares some similar features with that of the cuprates, both in terms of the symmetry and also in terms of having two-dimensional layers which are responsible for the electronic properties and which are doped by interleaving block layers. The interest on these systems principally resides in the onset at high temperature of a CDW broken symmetry ground state,[4] driven by a suitable FS nesting. Furthermore, the astonishing discovery of a pressure-induced superconductivity state in $CeTe_2$ below 2.7 K (Ref. 5) competing with a CDW phase [for which the critical temperature T_{CDW} has not yet been identified but is certainly well above 300 K (Refs. 4, 6, and 7)] and with a rather peculiar magnetic order ($T_N \sim 4.3$ K) (Ref. 8) lately attracted a lot of attention. Such an interplay makes the tellurides an ideal playground in order to investigate the electronic properties with respect to the competition between CDW, magnetic order, and superconductivity, and in a broader sense, the consequences of the electrons' confinement in the two-dimensional layeredlike structure, as well.

Recently, we have intensively investigated the RTe_3 and RTe_2 series by optical means.[9–11] Optical spectroscopic methods have been generally proven to be a powerful experimental tool in order to address the relevant absorption features associated with the CDW ground state.[2,3] Our first optical reflectivity data on RTe_3 (R=La, Ce, Nd, Sm, Gd, Tb, and Dy), collected over an extremely broad spectral range, allowed us to observe both the Drude component and the single-particle peak, which are ascribed to the contributions due to the free charge carriers and to the excitation across the

CDW gap, respectively.[9] We have then measured the pressure dependence of the optical reflectivity on $CeTe_3$ at 300 K (i.e., in the CDW state).[10] Upon increasing the externally applied pressure, the excitation due to the CDW gap decreases, in a quite equivalent manner when compressing the lattice by substituting large with small ionic radius rare-earth elements (i.e., by reducing the lattice constant a). Furthermore, the metallic (Drude) weight was found to be moderately enhanced with chemical pressure (i.e., along the rare-earth series). These results demonstrate that chemical and applied pressures similarly affect the electronic properties and equivalently govern the onset of the CDW state in RTe_3. The diminishing impact of the CDW condensate on the FS by reducing the lattice constant is actually the consequence of a quenching of the nesting conditions, driven by the modification of the electronic structure because of the lattice compression.[9,10]

The latest optical investigation of the related rare-earth ditellurides RTe_2 (R=La and Ce) confirms our previous findings on RTe_3.[11] We have extracted the energy for the CDW gap and found that the CDW collective state gaps a large portion of the Fermi surface. Moreover, it is worth mentioning that for both RTe_2 and RTe_3 series, we observed a high frequency power-law behavior in the optical conductivity (i.e., at energies larger than the CDW gap).[9,11] The latter result was found to be compatible with a scenario based on the Tomonaga-Luttinger liquid model for which direct electron-electron interactions and umklapp processes play a role in the electron dynamics at high energies.

While the single layer RTe_2 share several common features and similar properties with the related bilayer RTe_3 materials, there are also important differences. The lattice modulation is somewhat different for each member of the ditelluride family but is essentially identical for all members of the tritelluride family, being characterized in that case by a single unidirectional wave vector. Moreover, RTe_3 appears to be a line compound, whereas RTe_2 is known to have a substantial width of formation. As a consequence, while single crystals of RTe_3 do not exhibit sample-to-sample variation, there is an appreciable difference in the resistivity of single crystals of RTe_2 grown by different techniques[12,13] and to a much lesser extent even when taken from the same growth batch.[6] Variation in the superlattice modulation between different members of the RTe_2 family has been associated with the observation that the FS nesting wave vectors are somewhat poorly defined in comparison to RTe_3 and are therefore especially susceptible to perturbation, including the differences in the Te deficiency due to the width of the formation.[6] Hence, a systematic study aimed at determining the effect of chemical pressure on the CDW condensate is somewhat less meaningful than has been the case for RTe_3. In contrast, externally applied pressure has the distinct advantage of varying the lattice parameters for a single sample. This would enable a direct measure of the effect of compressing the lattice without any of the concerns associated with comparing the behavior of different members of the rare-earth series for which the Te deficiency might change substantially. Analogous to $CeTe_3$,[10] pressure-dependent optical investigations may be then of great relevance. It is instructive to establish a comparison between the physical properties of the two classes of rare-earth telluride compounds upon lattice compression.

In this paper, we present our optical results under externally applied pressure in $LaTe_2$. First, we introduce the investigated material along with the technical details pertaining to the experiment. The data presentation as well as their thorough analysis will be followed by a discussion, primarily focusing the attention on the comparison between the optical properties of the rare-earth polychalcogenides.

II. EXPERIMENT AND RESULTS

$LaTe_2$ single crystals were grown by slow cooling a binary melt so that they are as close to stoichiometry as possible.[6] As already anticipated above, $LaTe_2$ can be described in terms of a modulated Cu_2Sb-type structure ($P4/nmm$) and a superlattice modulation of the average structure has been observed via transmission electron microscopy (TEM) and x-ray diffraction.[4,6] Heat capacity measurements indicate that this material has a very small density of states at the Fermi level, while resistivity data show that it is far from being a good metal. Meanwhile, photoemission spectroscopy measurements of crystals produced by an alternative technique indicate that a substantial gap may exist on the entire FS.[14] Furthermore, the large anisotropy in the electrical resistivity confirms the low-dimensional character of the charge carriers.[6] Band structure calculations of the stoichiometric materials suggest a strongly anisotropic Fermi surface of mostly Te $5p$ character with minimal c-axis dispersion, large regions of which are nested.[15,16] Electron microprobe analysis, using elemental standards with an uncertainty of ± 0.03 in the Te content, determines the precise composition of $LaTe_{1.95}$ for the investigated specimen (which we will indicate as $LaTe_2$ throughout the rest of the paper). TEM patterns do not show any sample-to-sample variation, and optical conductivity data obtained at ambient pressure for several samples showed identical results.

A tiny piece of $LaTe_2$ (i.e., approximately 50×50 μm^2) was cut from the same well characterized specimen previously used in Ref. 11 and was placed on the top surface of a KBr pellet (acting as the pressure medium) presintered in the gasket hole of the pressure cell. The gasket was made of stainless steel, 50 μm thick under working conditions, and with a 200 μm diameter hole. A clamp-screw diamond anvil cell (DAC) equipped with high-quality type IIa diamonds (400 μm culet diameter) was employed for generating hydrostatic pressure up to 7 GPa. Pressure was measured with the standard ruby-fluorescence technique.[17]

Due to the metallic character of the sample, absorption measurements are not possible on this compound. Therefore, we carried out optical reflectivity measurements exploiting the high brilliance of the SISSI infrared beamline at Elettra synchrotron in Trieste.[18] We have investigated the ac plane of our sample with unpolarized light, since the search for a polarization dependent optical response always failed, supporting the optical isotropic nature of the ac plane. The incident and reflected light were focused and collected by a cassegrainian-based optical microscope equipped with a HgCdTe detector and coupled to a Bruker Michelson inter-

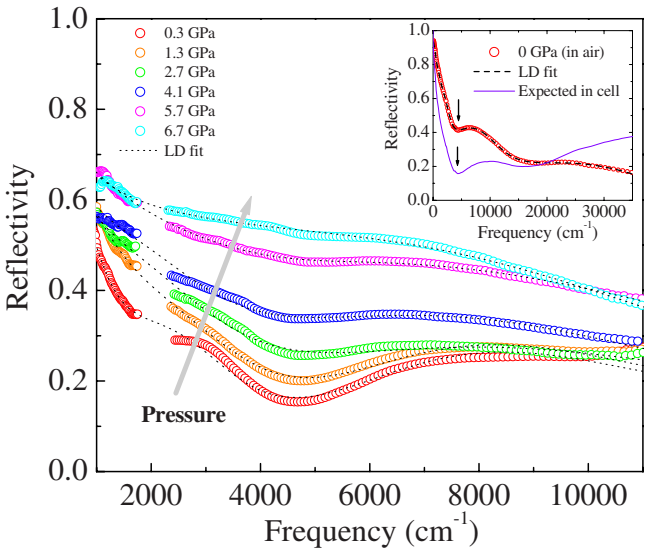

FIG. 1. (Color online) Pressure dependence of $R(\omega)$ in the mid-infrared spectral range of $LaTe_2$ at 300 K. The arrow indicates the trend of the reflectivity data upon increasing pressure. The $R(\omega)$ points in the energy interval of the diamond absorption (i.e., 1700–2300 cm^{-1}) have been omitted. The thin dotted lines are fits to the data within the Lorentz-Drude (LD) approach (see text). The inset displays the reflectivity spectrum measured in air from the far infrared up to the ultraviolet together with its LD fit which reproduces in great detail the measured $R(\omega)$ at ambient pressure (Ref. 11). The expected reflectivity inside the diamond anvil cell at zero pressure (Ref. 21) is reproduced as well. The arrow is here pointing out the depletion at about 5000 cm^{-1}, signaling the onset of the gap absorption.

ferometer with KBr and CaF_2 beam splitter, which allows us to explore the 600–11 000 cm^{-1} spectral range. In contrast to our previous optical study of $CeTe_3$ under pressure,[10] it was possible to obtain here high-quality spectra of the gasket. This has important implications, as discussed below, toward a robust determination of the reference signal and of the correct shape and value of the reflectivity inside the DAC. At each pressure, we therefore measured the light intensity reflected by the sample $I_S(\omega)$ and by the (steel) gasket $I_G(\omega)$, obviously at the diamond-specimen interface for both measurements. We thus obtain the quantity $R_G^S(\omega)=I_S(\omega)/I_G(\omega)$, so that $I_G(\omega)$ is acting here as the reference signal. Measuring the reflected intensity of the gasket at each pressure run allows us to monitor the variations in the light intensity due to the smooth depletion of the current in the synchrotron storage ring. The final spectra as a function of pressure were then achieved by multiplying each measured curve by a pressure-independent factor. This latter scaling factor is chosen in such a way so that the final spectra match with the expected $R(\omega)$ at zero pressure inside the cell. The expected $R(\omega)$ at ambient pressure of $LaTe_2$ (inset of Fig. 1) is calculated from the complex refractive index at zero pressure[11] and assuming the sample inside the DAC.[19–21] The resulting scaling factor is purely instrumental and corrects possible diffraction effects, which are induced by the nonperfectly flat shape of the sample as well as the underestimation of the reference steel signal. We furthermore emphasize that the reflectivity $R_G(\omega)=I_G(\omega)/I_{Au}(\omega)$ of steel (I_{Au} being the light intensity reflected by gold) is weakly frequency dependent in the spectral range of interest here. We have checked that the correction of $R_G^S(\omega)$ by R_G (i.e., $R_G^S R_G$) does not change the shape of the resulting final spectra, but just renormalizes them. In fact, the correction by R_G is already fully encountered by the subsequent rescaling of R_G^S to the expected reflectivity level inside the pressure cell (Fig. 1).

Figure 1 displays the pressure dependence of $R(\omega)$ between 10^3 and 1.1×10^4 cm^{-1}, where the strong diamond absorption around 2000 cm^{-1} has been cut out from the spectra, while its inset gives an overall view of $R(\omega)$ at ambient pressure as reproduced from Ref. 11. It is worth noting that the light spot was precisely limited (by means of apertures) to the sample area. In contrast to our first pressure-dependent optical investigation on $CeTe_3$,[10] the $R(\omega)$ spectra of $LaTe_2$ are remarkably smooth and do not display any evidence for interference pattern (between the diamond windows) because of diffused light. The low pressure $R(\omega)$ reproduces the depletion around 5000 cm^{-1}, already observed at ambient pressure (arrow in the inset of Fig. 1)[11] and ascribed to the onset of the CDW gap excitation. The striking feature in Fig. 1 is the progressive increase with increasing pressure of the reflectivity signal, accompanied by the filling in of the deep minimum in $R(\omega)$ at about 5000 cm^{-1}.

III. ANALYSIS

In order to extract the optical conductivity from the pressure-dependent reflectivity spectra, we must carry out a Kramers-Kronig (KK) analysis. The application of this method is, however, not trivial because the measured reflectivity spectra cover a limited frequency range, and the standard KK relation between the reflectivity and phase needs to be corrected when it is applied to the sample-diamond interface and the necessary correction term contains an *a priori* unknown parameter.[22,23]

For the KK analysis, the measured $R(\omega)$ on $LaTe_2$ needs first to be extrapolated to lower and higher frequencies and interpolated within the diamond absorption range (1700–2300 cm^{-1}). Figure 2 highlights the undertaken steps to achieve this goal. First of all, we recall that the complete absorption spectrum of $LaTe_2$ from the far infrared up to the ultraviolet at ambient pressure can be well reproduced within the Lorentz-Drude (LD) approach.[11] It consists in fitting the dielectric function by the following expression:[19,20]

$$\tilde{\epsilon}(\omega) = \epsilon_1(\omega) + i\epsilon_2(\omega) = \epsilon_\infty - \frac{\omega_p^2}{\omega^2 + i\omega\gamma_D} + \sum_j \frac{S_j^2}{\omega_j^2 - \omega^2 - i\omega\gamma_j}, \quad (1)$$

where ϵ_∞ is the optical dielectric constant and ω_p and γ_D are the plasma frequency and the width of the Drude peak, whereas ω_j, γ_j, and S_j^2 are the center-peak frequency, the width, and the mode strength for the jth Lorentz harmonic oscillator (HO), respectively. The knowledge of $\tilde{\epsilon}(\omega)$ gives us the access to all optical functions and finally allows us to reproduce the measured $R(\omega)$ spectra. The optical properties of RTe_2 at ambient pressure are well described by one Drude

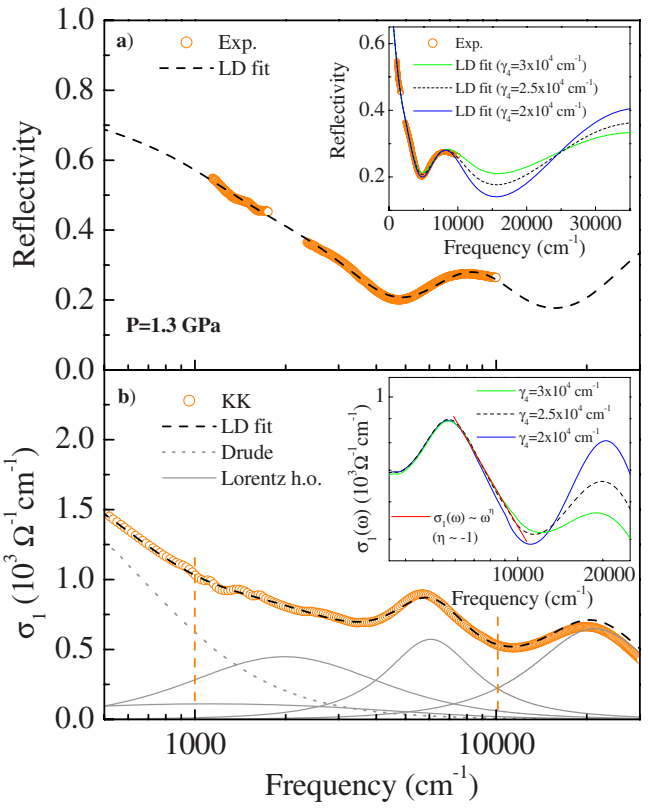

FIG. 2. (Color online) (a) Measured $R(\omega)$ of $LaTe_2$ at 1.3 GPa and its extension based on the LD fit (see text). (b) Real part $\sigma_1(\omega)$ of the complex optical conductivity achieved through Kramers-Kronig (KK) transformation of the spectrum in panel (a) and its reproduction within the LD fit. The fit components are displayed as well. The dashed vertical lines in panel (b) highlight the spectral range, where the original $R(\omega)$ data were collected. The inset in panel (a) shows the three different extrapolations of $R(\omega)$ at high frequencies (see text), while the inset in panel (b) reproduces the corresponding $\sigma_1(\omega)$, plotted on a bilogarithmic scale. The power-law behavior $[\sigma_1(\omega) \sim \omega^\eta]$ at frequencies above 6000 cm^{-1} is unaffected by the various extrapolations and $\eta \sim -1$ with a variation of about ± 0.1 for the three extrapolations.

term for the metallic component and three Lorentz HOs accounting for the broad midinfrared feature, then ascribed to the single-particle peak excitation. One additional HO is also considered in the fit procedure in order to mimic the onset of the electronic interband transitions (see the inset of Fig. 2 in Ref. 11). The fit quality over the entire spectral range is remarkably good, as shown in the inset of Fig. 1, for our $LaTe_2$ sample.[11]

Using the same number of fit components as at ambient pressure,[11] we can also reproduce the $R(\omega)$ spectra under pressure. We directly fit $R(\omega)$ in the measured spectral range (Fig. 1) using Eq. (1) and obviously accounting for the sample inside the DAC.[21] Even though we address a limited energy interval, we are able to achieve a rather precise fit of $R(\omega)$ as a function of pressure (thin dotted lines in Fig. 1). This phenomenological approach also enables us to extrapolate the $R(\omega)$ spectra beyond the experimentally available energy range and to even interpolate $R(\omega)$ in the energy region of the diamond absorption. Such an extrapolation at

TABLE I. Pressure dependence of the reflectivity energy pole ω_β, the single-particle peak ω_{SP}, the plasma frequency ω_p, the fraction Φ of the ungapped Fermi surface, and the power-law exponent η.

P (GPa)	ω_β (cm^{-1})	ω_{SP} (cm^{-1})	ω_p (cm^{-1})	Φ	η
0.3	8000	4754	7656	0.16	−1.1
1.3	8500	4206	8953	0.21	−1.0
2.7	9600	4316	9053	0.16	−0.7
4.1	9800	3528	10510	0.22	−0.8
5.7	12350	2425	14000	0.26	−1.0
6.7	11500	2285	15000	0.36	−1.0

lower and higher energies is shown, as an example, for the data at 1.3 GPa in Fig. 2(a). The related optical conductivity $\sigma_1(\omega)$ at 1.3 GPa, calculated within the Lorentz-Drude fit, is displayed in Fig. 2(b) along with its own fit components.

The precise shape of $\sigma_1(\omega)$ and its peculiar frequency dependence, including the possible power-law behavior at high frequencies discussed below, are sensitively governed by subtle changes of the measured $R(\omega)$. The Lorentz-Drude reconstruction of $\sigma_1(\omega)$ is then not enough, since $\sigma_1(\omega)$ calculated within this phenomenological method might suffer to some extent from the constraints, which are imposed by the use of the Lorentz HOs. We therefore perform reliable KK transformations, following the procedure successfully employed by Pashkin *et al.* for the organic Bechgaard salt $(TMTTF)_2AsF_6$.[22] The KK relation for the phase ϕ of the reflectivity $R(\omega)$ has the following form:[23,24]

$$\phi(\omega_0) = -\frac{\omega_0}{\pi} P \int_0^{+\infty} \frac{\ln R(\omega)}{\omega^2 - \omega_0^2} d\omega + \left[\pi - 2 \arctan \frac{\omega_\beta}{\omega_0} \right], \tag{2}$$

where ω_β is the position of the reflectivity pole on the imaginary axis in the complex frequency plane. In the case of measurements on the sample-air interface, ω_β tends toward infinity and the second term vanishes. For the sample-diamond interface, the second term must, however, be taken into account. The criterion for the proper value of ω_β is the agreement between the optical conductivity obtained by the KK analysis and that from the initial fit.[22]

Figure 2(b) well illustrates the self-consistency of the applied data analysis for the 1.3 GPa data. The comparison between the $\sigma_1(\omega)$ spectra, obtained first through KK transformation of the extended $R(\omega)$ data of Fig. 2(a) and second from the direct Lorentz-Drude fit, is indeed astonishingly good and well emphasizes the reliability of this procedure. Table I summarizes for all studied pressures the ω_β values, which allow the best agreement between the Lorentz-Drude calculation of $\sigma_1(\omega)$ and the output of the KK transformations.

We also took good care to check the effect of the high frequency extrapolations of the measured $R(\omega)$, a rather sensitive issue when applying the KK analysis. The inset of Fig. 2(a) shows $R(\omega)$ at 1.3 GPa with three different extrapola-

tions, which have been *ad hoc* manipulated by changing the width of the fourth HO at $\omega_4 \sim 1.2 \times 10^4$ cm^{-1}. The first extrapolation considers $\gamma_4 = 2.5 \times 10^4$ cm^{-1} for the fourth HO, which also corresponds to the best fit of the measured $R(\omega)$ [dashed line in the main panel of Fig. 2(a)]. The other two extrapolations were obtained with $\gamma_4 = 2 \times 10^4$ and 3×10^4 cm^{-1}, respectively.[25] The resulting altered $R(\omega)$ at high frequencies smoothly joins the rest of the (measured) $R(\omega)$ signal at about 10^4 cm^{-1}. The inset of Fig. 2(b) compares the real part $\sigma_1(\omega)$ of the complex optical conductivity obtained by the KK transformations of the $R(\omega)$ spectra with the three different extrapolations [inset of Fig. 2(a)]. Due to the rather local character of the KK transformations, the final result is less affected by the extrapolations of $R(\omega)$ at frequencies above 10^4 cm^{-1} and their impact on the frequency dependence of $\sigma_1(\omega)$ below 10^4 cm^{-1} is very moderate. The $\sigma_1(\omega)$ spectra are almost identical and start to deviate from each other at the very upper end of the measured spectral range. This also means that we can trust our data and the corresponding KK analysis all the way up to the high frequency limit of about $\omega \sim 1.1 \times 10^4$ cm^{-1} reached in our experiment. We have also considered other (more crude) routes to artificially extrapolate $R(\omega)$ at high frequencies (e.g., by simply multiplying the spectra above 10^4 cm^{-1} by a factor), reaching, however, similar conclusions.

IV. DISCUSSION

The optical conductivity at all measured pressures is shown in Fig. 3 in the spectral range $2 \times 10^3 \leq \omega \leq 1.2 \times 10^4$ cm^{-1}, which essentially lies within the energy interval [vertical dashed lines in Fig. 2(b)] covered by the measurement of $R(\omega)$ under pressure. Particularly at low pressures, two main features are immediately well recognized: the low frequency spectral weight and the midinfrared absorption, peaked at about 6000 cm^{-1}. Indeed, the finite optical conductivity below 3000 cm^{-1} signals the onset of an effective metallic contribution, which is associated with the Drude response. According to the arguments and experimental evidence presented in Ref. 11, we ascribe the midinfrared absorption to the single-particle peak excitation across the CDW gap. The application of pressure causes a gradual shift of the midinfrared feature to lower frequencies in $\sigma_1(\omega)$, so that it progressively merges into the high frequency tail of the metallic (Drude) response. This pairs with the already anticipated behavior of $R(\omega)$ (Fig. 1), where the depletion at about 5000 cm^{-1} disappears with increasing pressure. The trend in $\sigma_1(\omega)$ bears a striking similarity with what has been recognized in previous data about the chemical and applied pressure dependence of the optical properties in the related $R\mathrm{Te}_3$ compounds.[9,10]

It is instructive to extract the relevant energy scales shaping the absorption spectrum: the single-particle peak frequency ω_{SP}, due to the excitations across the CDW gap, and the Drude plasma frequency ω_p. To this end, we exploit the output of the Lorentz-Drude fit to our spectra described above. In our previous investigation of the pressure dependence of $R(\omega)$ in CeTe_3,[10] we failed to collect data below the diamond absorption at about 2000 cm^{-1}. In LaTe_2, on the contrary, we could extend the measurable spectral range of $R(\omega)$ even in the interval between 1000 and 1700 cm^{-1}. This helps in order to better pin down the fit of the Drude component to the measured data set, allowing this way a more realistic estimation of ω_p under pressure. Consequently, the Lorentz-Drude fit permits us to establish how the spectral weight (which is proportional to ω_p^2 for the Drude term and to S_j^2 for the Lorentz HO) is distributed among the various components [Figs. 2(b) and 3]. The plasma frequency ω_p is listed in Table I.

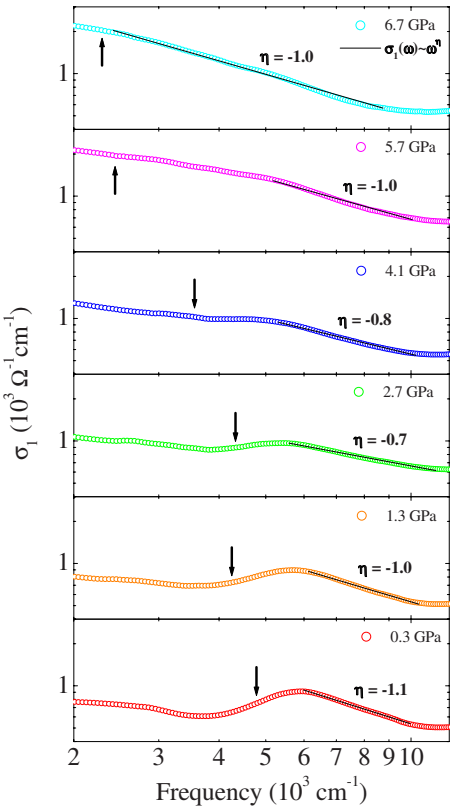

FIG. 3. (Color online) Real part $\sigma_1(\omega)$ of the complex optical conductivity of LaTe_2 at various pressures plotted on a bilogarithmic scale. The arrows indicate the position of ω_{SP} [Eq. (3)]. The power-law behavior [$\sigma_1(\omega) \sim \omega^{\eta}$] is also displayed with the resulting exponent η.

Analogous to our recent optical investigations on $R\mathrm{Te}_2$ and $R\mathrm{Te}_3$,[9–11] we then define the average weighted energy ω_{SP} as follows:

$$\omega_{SP} = \frac{\sum_{j=1}^{3} \omega_j S_j^2}{\sum_{j=1}^{3} S_j^2}. \tag{3}$$

The sum is over the first three HOs. Here, ω_{SP} is reported in Table I,[26] and its position is also indicated by the arrows in Fig. 3. The decrease in ω_{SP} with pressure confirms the qualitative observation, made above, about the merging of the midinfrared feature into the Drude component of $\sigma_1(\omega)$. It is worthwhile to compare the pressure dependence of ω_{SP} for

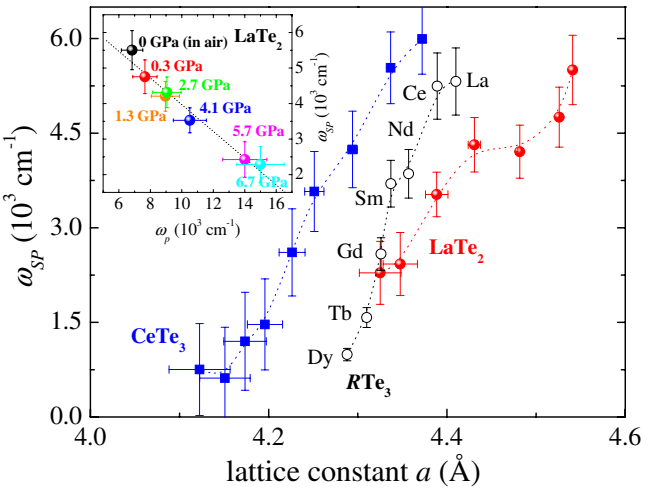

FIG. 4. (Color online) Single-particle peak energy ω_{SP} as a function of the lattice constant a for $LaTe_2$, $CeTe_3$ (Ref. 10), and the RTe_3 series (Ref. 9). Inset: single-particle peak energy ω_{SP} versus plasma frequency ω_p for $LaTe_2$ as a function of pressure. Pressure is here an implicit variable.

$LaTe_2$ with that of $CeTe_3$.[10] Such a comparison is shown in Fig. 4, which also displays ω_{SP} for the rare-earth tritelluride series (i.e., chemical pressure).[9] To allow this comparison, we plot ω_{SP} as a function of the lattice constant a. We note that since the pressure dependence of the lattice parameters of $LaTe_2$ is not known, we must rely on the crude but effective approach based on the Murnaghan equation,[27,28] already applied for $CeTe_3$.[10] It is quite evident that by compressing the lattice, there is a progressive reduction in ω_{SP}.[9,10] The close similarity in the pressure dependence of the optical properties of RTe_2 and RTe_3 indicates that pressure affects the electronic structure of these two sets of compounds similarly, irrespective of whether the materials contain single or double Te layers. Consequently, the striking variation in T_{CDW} across the rare-earth series for RTe_3 (Ref. 29) cannot be attributed primarily to variation in the bilayer splitting of the FS as a consequence of chemical pressure. In that case, one would anticipate a more dramatic variation with respect to applied pressure for the RTe_3 compounds than for RTe_2, which is not observed.

The suppression of ω_{SP} upon reducing the lattice constant is also accompanied by an enhancement of the plasma frequency ω_p. This is shown in the inset of Fig. 4, noting that the linear interpolation is here meant as a guide for the eyes, while pressure is obviously an implicit variable. These findings emphasize that pressure affects the electronic structure in such a way as to reduce the impact of the CDW condensate. The decrease in ω_{SP} upon compressing the lattice concomitantly occurs with the release of itinerant charge carriers (inset of Fig. 4), which therefore increases the effective Drude weight (i.e., the plasma frequency).

Further support to the above considerations comes from the sum rule arguments. Following indeed the well-established concept about the spectral weight distribution, introduced in our previous work on $NbSe_3$ (Ref. 30) and then successfully applied on RTe_2 and RTe_3 as well,[9,11] we can define the ratio,

$$\Phi = \frac{\omega_p^2}{\omega_p^2 + \sum_{j=1}^{3} S_j^2}, \tag{4}$$

between the Drude weight in the CDW state and the total spectral weight of the hypothetical normal state. This latter quantity is achieved by assuming that above T_{CDW} the weight of the single-particle peak (i.e., $\Sigma_{j=1}^{3} S_j^2$) merges together with the Drude weight. Equation (4) tells us how much of FS survives in the CDW state and is not gapped by the formation of the CDW condensate. Φ is displayed in Table I and turns out to generally increase upon compressing the lattice. This increase in Φ with pressure is pretty much in trend with results on RTe_2 (Ref. 11) and RTe_3 (Ref. 9) and emphasizes the lesser impact of the CDW on the FS upon reducing the lattice constant.

The extension, achieved here, of the measurable spectral range up to 1.1×10^4 cm^{-1} is of great relevance for the assessment of the pressure dependence of the power-law behavior in $\sigma_1(\omega)$ at $\omega \geq \omega_{SP}$. Figure 3 reports the best power law $\sigma_1(\omega) \sim \omega^{\eta}$ of $LaTe_2$ under pressure in the spectral range above the CDW gap absorption. The exponents η are summarized in Table I, with an estimation error of about ± 0.1. The values of η are very close to -1, which compare fairly well with the previous results on $LaTe_2$ and $CeTe_2$,[11] as well as on the RTe_3 series at ambient pressure.[9] Even though we seek the largest energy interval, for which such a power law in $\sigma_1(\omega)$ applies, in most cases though, it is appropriate for an energy range extending over less than a decade. This means that caution should be placed on the power-law behavior given the rather small frequency interval over which it is extracted. Nonetheless, the power law in $\sigma_1(\omega)$ is found within the spectral range originally covered by the $R(\omega)$ measurements and it is independent of any extrapolation effects of $R(\omega)$. This is clearly demonstrated in the inset of Fig. 2(b), where the power-law behaviors in $\sigma_1(\omega)$ for the three different extrapolations of $R(\omega)$ [inset of Fig. 2(a)] are, in fact, almost identical, giving the exponent $\eta \sim -1.0 \pm 0.1$.

Power-law behaviors are expected in a wealth of physical quantities, when confining electrons in low dimensions and considering the effects of interactions. This occurs particularly in one dimension because the direct electron-electron interaction is indeed unavoidable and the quasiparticle concept breaks down. The appropriate theoretical framework is based on the Tomonaga-Luttinger liquid scenario, for which the exponent η of the power law is a measurement of the strength of interactions.[31,32] The clearest optical evidence for a Tomonaga-Luttinger liquid behavior has been achieved so far in the prototype one-dimensional organic Bechgaard salts.[33,34] A similar power-law decay of $\sigma_1(\omega)$, as seen in the organics at energies larger than the gap, is also predicted for the CDW state. If the Tomonaga-Luttinger liquid scenario is applicable to the rare-earth tellurides, it would give evidence for direct interaction between electrons, as the source of umklapp scattering,[31,32] and would imply the non-negligible contribution of 1D correlation effects in the physics of these low-dimensional systems.[31,32] The analogy between the power-law behaviors of $LaTe_2$ and of the rare-earth tritellu-

ride series may hint in both cases to a (hidden) one-dimensional character of the electronic properties at high energies, despite their two-dimensional structure.[9,35] Moreover, values of η of about -1 would indicate that the rare-earth tellurides are close to the weakly interacting limit within the Tomonaga-Luttinger liquid framework.[36] The most puzzling finding, however, is the rather negligible pressure dependence of η in $LaTe_2$. This would suggest that (1D) correlation effects do not change dramatically upon compressing the lattice. For the range of pressures considered, we might even speculate that compressing the lattice does not induce any remarkable dimensionality crossover.

V. CONCLUSIONS

We have reported the optical response of $LaTe_2$ under externally applied pressure, focusing our attention on the single-particle peak excitation across the CDW gap. We were able to cover a rather large spectral range in the midinfrared and to reach high pressures of up to 7 GPa. These are important prerequisites in order to establish the progressive closing of the CDW gap and the enhancement of the Drude weight upon compressing the lattice. The investigated spectral range is broad enough to allow furthermore educated guesses on the issue to which extent the applied pressure may influence the effect of electron-electron interactions. It turns out that lattice compression moderately affects the electronic correlations in $LaTe_2$.

ACKNOWLEDGMENTS

The authors wish to thank J. Müller for technical help and T. Giamarchi for fruitful discussions. One of us (A.S.) wishes to acknowledge financial support from the Della Riccia Foundation. This work has been supported by the Swiss National Foundation for Scientific Research and by the NCCR MaNEP pool. This work is also supported by the Department of Energy, Office of Basic Energy Sciences under Contract No. DE-AC02-76SF00515.

[1] R. Peierls, *Quantum Theory of Solids* (Clarendon, Oxford, 1955).
[2] G. Grüner, *Density Waves in Solids* (Addison-Wesley, Reading, MA, 1994).
[3] *Strong Interactions in Low Dimensions*, edited by D. Baeriswyl and L. Degiorgi (Kluwer, Dordrecht, 2004).
[4] E. DiMasi, B. Foran, M. C. Aronson, and S. Lee, Phys. Rev. B **54**, 13587 (1996).
[5] M. H. Jung, A. Alsmadi, H. C. Kim, Y. Bang, K. H. Ahn, K. Umeo, A. H. Lacerda, H. Nakotte, H. C. Ri, and T. Takabatake, Phys. Rev. B **67**, 212504 (2003).
[6] K. Y. Shin, V. Brouet, N. Ru, Z. X. Shen, and I. R. Fisher, Phys. Rev. B **72**, 085132 (2005), and references therein.
[7] J.-S. Kang, C. G. Olson, Y. S. Kwon, J. H. Shim, and B. I. Min, Phys. Rev. B **74**, 085115 (2006).
[8] M. H. Jung, T. Ekino, Y. S. Kwon, and T. Takabatake, Phys. Rev. B **63**, 035101 (2000).
[9] A. Sacchetti, L. Degiorgi, T. Giamarchi, N. Ru, and I. R. Fisher, Phys. Rev. B **74**, 125115 (2006).
[10] A. Sacchetti, E. Arcangeletti, A. Perucchi, L. Baldassarre, P. Postorino, S. Lupi, N. Ru, I. R. Fisher, and L. Degiorgi, Phys. Rev. Lett. **98**, 026401 (2007).
[11] M. Lavagnini, A. Sacchetti, L. Degiorgi, K. Y. Shin, and I. R. Fisher, Phys. Rev. B **75**, 205133 (2007).
[12] Y.-S. Kwon and B.-H. Min, Physica B **281-282**, 120 (2000).
[13] M.-H. Jung, B.-H. Min, Y.-S. Kwon, I. Oguro, F. Iga, T. Fujita, T. Ekino, T. Kasuya, and T. Takabatake, J. Phys. Soc. Jpn. **69**, 937 (2000).
[14] D. R. Garcia, G.-H. Gweon, S. Y. Zhou, J. Graf, C. M. Jozwiak, M. H. Jung, Y. S. Kwon, and A. Lanzara, Phys. Rev. Lett. **98**, 166403 (2007).
[15] J. Laverock, S. B. Dugdale, Zs. Major, M. A. Alam, N. Ru, I. R. Fisher, G. Santi, and E. Bruno, Phys. Rev. B **71**, 085114 (2005).
[16] A. Kikuchi, J. Phys. Soc. Jpn. **67**, 1308 (1998).
[17] H. K. Mao, J. Xu, and P. M. Bell, J. Geophys. Res. **91**, 4673 (1986).
[18] S. Lupi, A. Nucara, A. Perucchi, P. Calvani, M. Ortolani, L. Quaroni, and M. Kiskinova, J. Opt. Soc. Am. B **24**, 959 (2007).
[19] F. Wooten, *Optical Properties of Solids* (Academic, New York, 1972).
[20] M. Dressel and G. Grüner, *Electrodynamics of Solids* (Cambridge University Press, Cambridge, 2002).
[21] The reflection coefficient for the experimental arrangement given by the sample and the diamond window of the DAC is defined by $\hat{r}=(n'-\hat{n})/(n'+\hat{n})$ (Ref. 20), $n'=2.42$ being the refractive index of diamond [P. Dore, A. Nucara, D. Cannavo', G. De Marzi, P. Calvani, A. Marcelli, R. S. Sussmann, A. J. Whitehead, C. N. Dodge, A. J. Krehan, and H. J. Peters, Appl. Opt. **37**, 5731 (1998)] and $\hat{n}$ the complex refractive index of $LaTe_2$ (Ref. 11).
[22] A. Pashkin, M. Dressel, and C. A. Kuntscher, Phys. Rev. B **74**, 165118 (2006).
[23] J. S. Plaskett and P. N. Schatz, J. Chem. Phys. **38**, 612 (1963).
[24] R. D. McDonald, Ph.D. thesis, Magdalen College, 2001.
[25] The change of γ_4 implies a minor adjustment of the parameters of S_3^2 and γ_3 (strength and damping) of the third Lorentz HO, leaving, however, the other ones unchanged. Apart from the obvious changes of $R(\omega)$ above the upper limit of our measurement, the fit quality of $R(\omega)$ remains outstanding in the measured spectral range.
[26] The single-particle peak frequency ω_{SP} [Eq. (3)] does not change significantly as a consequence of the three extrapolations of $R(\omega)$ [inset of Fig. 2(a)] (Ref. 25). The same applies for the plasma frequencies ω_p, which are totally unaffected by the shape of $R(\omega)$ at high frequencies.
[27] F. D. Murnaghan, Proc. Natl. Acad. Sci. U.S.A. **30**, 244 (1944).
[28] From the phononic term βT^3 in the specific heat [$\beta=8\times10^{-4}$ J/mol K^4 (Ref. 6)], we extract the bulk modulus $B_0=\rho v_s^2=29.3$ GPa, with v_s being the sound velocity. Assuming the linear pressure dependence of $B(P)$, it follows that the pressure dependence of the volume $V(P)$ is achieved through $V(P)$

$=V(0)(1+\frac{B'}{B_0}P)^{-1/B'}$ (Ref. 27), with B' varying between 4 and 8. The pressure dependence of the lattice constant is then $a(P)=a(0)[V(P)/V(0)]^{1/3}$, considered as the average between the estimation of $V(P)$ for $B'=4$ and 8 (Ref. 10).

[29] N. Ru, C. L. Condron, G. Y. Margulis, K. Y. Shin, J. Laverock, S. B. Dugdale, M. F. Toney, and I. R. Fisher, Phys. Rev. B **77**, 035114 (2008).

[30] A. Perucchi, L. Degiorgi, and R. E. Thorne, Phys. Rev. B **69**, 195114 (2004).

[31] T. Giamarchi, *Quantum Physics in One Dimension* (Oxford University Press, Oxford, 2004).

[32] T. Giamarchi, Chem. Rev. (Washington, D.C.) **104**, 5037 (2004).

[33] V. Vescoli, L. Degiorgi, W. Henderson, G. Grüner, K. P. Starkey, and L. K. Montgomery, Science **281**, 1181 (1998).

[34] A. Schwartz, M. Dressel, G. Grüner, V. Vescoli, L. Degiorgi, and T. Giamarchi, Phys. Rev. B **58**, 1261 (1998).

[35] Since the Te planes are composed of equivalent orthogonal chains, there is no way to avoid the possible contribution from the perpendicular hopping. It is nevertheless reasonable to expect that the parallel contribution is dominant.

[36] We note that the exponent η for a one-dimensional band insulator would be totally different, ranging between −2, when coupling to phonons is included, and −3, when the lattice is assumed to be rigid and only umklapp scattering off the single-period lattice potential is possible [V. Vescoli, F. Zwick, J. Voit, H. Berger, M. Zacchigna, L. Degiorgi, M. Grioni, and G. Gruner, Phys. Rev. Lett. **84**, 1272 (2000)]. Our exponents η are, moreover, different from the expectation in the case of the decay of $\sigma_1(\omega)$ due to the high frequency tail of a single Lorentzian, for which η is equal to −2.